



## Contact-free wheat mildew detection with commodity wifi

Pengming Hu<sup>a</sup>, Weidong Yang<sup>a,\*</sup>, Xuyu Wang<sup>b</sup>, Shiwen Mao<sup>c,1</sup>

<sup>a</sup> College of Information Science and Engineering, Henan University of Technology, Zhengzhou, 450001, People's Republic of China

<sup>b</sup> Department of Computer Science, California State University, Sacramento, CA 95819-6021, USA

<sup>c</sup> Department of Electrical and Computer Engineering, Auburn University, Auburn, AL 36849-5201, USA

### ARTICLE INFO

#### Keywords:

Channel state information (CSI)  
 Commodity wifi  
 Wheat mildew detection  
 K-Means clustering  
 Machine learning

### ABSTRACT

Mildew is recognized as one of the most critical causes of the damages in food storage. Due to the complex operation and high cost, many advanced detection instruments cannot be widely deployed, while the detection of grain mildew are mostly carried out manually (i.e., inspection by experts) nowadays with very low efficiency. To address this problem, we present a non-destructive, non-intrusive, and low-cost mildew detection system for stored wheat implemented with off-the-shelf WiFi devices, which represents a new application of the Internet of Things (IoT) for smart agriculture. In this paper, we introduce the impact of wheat mildew in stored food, and demonstrate that it is viable to utilize WiFi Channel State Information (CSI) amplitude for detection of mildew in stored wheat. Next, we propose the MiFi system, which comprises sensing of WiFi CSI data, data preprocessing, a radial basis function (RBF) neural network-based detection model, and mildew detection. We conduct extensive experiments to validate the performance of the proposed MiFi system using real grain samples. The results show that MiFi achieves an average detection accuracy of over 90% in both line-of-sight (LOS) and non-line-of-sight (NLOS) scenarios, as well as a comparable detection performance as manual detection by an expert.

### 1. Introduction

The world's population is fast growing and the people's quality of life is being improved. These both put every increasing demands and requirements on the quantity and quality of food such as wheat and grain Hu et al. (2019); Vasisht et al. (2017). Although the annual production of food over the world has exceeded 2 billion tons recently Jayas (2012), considerable amount of food is lost due to the damage incurred during the storage process, since the produced food are not to be consumed immediately and sometimes the food needs to be stored for a few years. Among many factors, wheat mildew can lead to considerable loss of both wheat processing quality and nutritional quality, and even leads to fungal contamination in many cases Lanier et al. (2010). Usually farmers and distributors lack the necessary professional knowledge and do not have access to the high-cost testing equipment. Therefore, they are not able to test the status of stored food on a timely basis, except for inspecting the food samples and judge by experience. Rapid detection of mildew in grain is important to achieve efficient and secure food storage, and to reduce the waste incurred during the storage process and reduce the cost of food.

However, detection mildew in stored grain is a challenging problem. The present approach for detection of mildew in stored grain is largely done manually, i.e., inspection by an expert. That is, the level of grain mildew is determined by visual inspection and the olfactory experience of the inspector. Such a manual approach is usually inefficient and unreliable, since it depends on the subjective judgment of the expert. With the advance of the Internet of Things (IoT), various sensors and expensive instruments have been developed for detection of grain mildew, including electronic nose sensors Zhang et al. (2007); Zhao et al. (2008), near infrared spectroscopy Fernández-Ibañez et al. (2009), image processing Hong et al. (2007); Zhong-zhi et al. (2010), among others. Although being effective, the wide deployment of these techniques is hindered by the relatively high cost and the complex operation. Consequently, non-intrusive, low-cost, fast and accurate detection of wheat mildew is in great demand.

WiFi is a dominant wireless communications technology to serve mobile users. The physical layer (PHY) of the WiFi standard incorporates Orthogonal Frequency-Division Multiplexing (OFDM) to combat the severe propagation impairments in indoor environments, such as multi-

\* Corresponding author.

E-mail addresses: [huhelai007@163.com](mailto:huhelai007@163.com) (P. Hu), [yangweidong@haut.edu.cn](mailto:yangweidong@haut.edu.cn) (W. Yang), [xuyu.wang@csus.edu](mailto:xuyu.wang@csus.edu) (X. Wang), [smao@ieee.org](mailto:smao@ieee.org) (S. Mao).

<sup>1</sup> This work was presented in part at IEEE GLOBECOM 2019 [1]. This work was supported in part by the National Key Research and Development Program of China (2017YFD0401001), the Program for Science & Technology Innovation Talents in Universities of Henan Province (19HASTIT027), the Fundamental Research Funds for Henan Provincial Colleges and Universities (2018RCJH12), the NSFC (61772173), and the NSF (ECCS-1923163, CNS-2107190, and CNS-2105416).

path propagation and frequency-selective fading. For some commercial network interface cards (NIC) of WiFi, open-source device drivers have been developed, which enables the receiver to obtain channel state information (CSI) from each received WiFi packet. For instance, the Intel 5300 NIC Halperin et al. (2010) can provide amplitude and phase readings for 30 subcarriers, and the Atheros 9kth NIC Xie et al. (2018) can the CSI samples for 56 subcarriers over a 20 MHz band channel for each received packet. Unlike received signal strength (RSS), CSI is a fine-grained channel model that better captures the features of the propagation environment that the WiFi packet has experienced, e.g., attenuation, distortion, and the multipath effect. Unlike RSS, CSI samples are usually more stable, and consequently, they have utilized in many RF sensing applications Jiang (2018); Wang et al. (2018), such as human vital sign estimation Wang et al. (2021b, 2017e) and indoor fingerprinting Wang et al. (2017b).

In this paper, we propose to leverage WiFi CSI for contact-free wheat mildew detection. The goal is to develop a low-cost, non-intrusive, and automated mildew monitoring system for stored grain. The development of mildew in store grain usually involves physiological changes in a number of external and internal states. When a WiFi signal propagates through the grain, such physiological change will cause considerable and measurable changes in the received signal, as reflected in the corresponding CSI samples. Through extensive experiments with real stored grain samples, we validate this hypothesis, where three types of mildew states are tested, including normal samples, samples in the initial stage of mildew, and samples in the complete mildew stage. It is demonstrated that there is slight differences in CSI amplitude between normal samples and initial mildew stage samples, and significant differences in CSI amplitude between initial mildew stage samples and completely mildewed samples. Our experiments justify the feasibility of leveraging WiFi CSI data for detection of wheat mildew.

Specifically, we present the design of the MiFi system, a device-free wheat Mildew detection system with WiFi CSI amplitude data. The proposed system comprises a sensing module, a preprocessing module, a detection modeling module, and a mildew detection module. CSI amplitude samples are first measured in the sensing module. The preprocessing module is to calibrate the CSI data using a Hampel identifier, environmental noise remover, and by subcarrier selection and normalization. The Hampel identifier is used to eliminate outliers in the measured raw data, and the Butterworth filter is applied to eliminate the ambient noise in the raw data. The most sensitive subcarrier is then selected according to a mean absolute deviation algorithm. Finally, the CSI amplitude samples on the selected subcarrier is normalized. In the detection modeling module, a *Radial Basis Function (RBF) neural network* is utilized for mildew detection using the calibrated CSI amplitude data. The *K*-means clustering algorithm is applied to determine the parameter setting of the RBF neural network model. The overall goal is to develop a simple and fast system for rapid determination of the mildew level in stored wheat. The use of radial basis function and K-means clustering has the desirable characteristics of low computational complexity, fast convergence, and better results, which is important to achieve rapid wheat mildew detection. In the last detection module, the wheat mildew level is estimated using a *classification matrix* through a combination of linear (i.e., the output layer) and non-linear (i.e., the Gaussian kernel) RBF neural networks.

The main contributions made in this paper are summarized in the following.

- Through an extensive experimental study, this paper verifies the feasibility of leveraging WiFi CSI amplitude data for detection the mildew of stored gain. Our results demonstrate that the WiFi CSI can capture the physiological variations caused by different mildew states when propagating through wheat samples, and thus can be used to distinguish different wheat mildew states.
- We present the MiFi system design, composed of (i) a sensing module that measure the WiFi CSI data; (ii) a preprocessing module that

calibrates raw CSI amplitude data; (iii) a detection modeling module with a novel RBF neural network based learning method; and (iv) a mildew detection module. To the best of our knowledge, this is the first work that applies WiFi based RF sensing for non-intrusive wheat mildew detection.

- We implement the proposed MiFi system using off-the-shelf WiFi devices and carry out extension experiments to validate its performance with real wheat samples. Our experimental results show that MiFi can achieve an average detection accuracy of over 90% in both line-of-sight (LOS) and non-line-of-sight (NLOS) scenarios, as well as a comparable detection performance as manual detection by an expert.

In the rest of this paper, we present the background and our feasibility study in Section 2. The MiFi system design is elaborated in Section 3 and evaluated in Section 4. Section 5 reviews related work and Section 6 concludes this paper.

## 2. Preliminaries and feasibility study

### 2.1. Wheat mildew detection: State-of-the-Art

Mildew is very harmful for stored wheat, since it causes pollution of stored food, loss of nutrients, as well as food-borne diseases. Microbial and environmental factors are the main causes of mildew development in stored wheat. Mildew is usually caused by the microbes in wheat granules during harvesting and by the granary microorganisms during storage Magan and Aldred (2007). In addition, wheat mildew is also affected by granary type, temperature, humidity, and other environmental factors during storage Nithya et al. (2011). If timely measures are taken, the wheat in the early stage of mildew can still be used. However, completely mildewed wheat will not be useful and should be destroyed as soon as possible to avoid further damage such as causing human diseases. A low-cost and non-destructive detection system of wheat mildew state will be helpful for avoiding losses in foot storage.

In this paper, we propose to detect the mildew state of stored grain by passing WiFi signals through grain samples. This is achieved by analyzing the received WiFi signal, after it passing through the grain samples, to learn the characteristics of the WiFi channel with respect to shadowing fading, reflection, and small-scale fading. To model the impact of mildew state on the received WiFi signal (or the WiFi channel), the concept of *dielectric constant* can be used as an indicator of the wheat mildew state. The complex relative permittivity  $\epsilon^*$  of a material in the frequency domain is given by Komarov et al. (2005)

$$\epsilon^* = \epsilon' - j\epsilon'' \quad (1)$$

The real part  $\epsilon'$  in (1) is the dielectric constant, which represents the ability of the material to store energy of the electric field; and the imaginary part  $\epsilon''$  is a dielectric loss factor, which usually indicates the ability of a material to consume electrical energy. Thus these factors affect the attenuation and absorption of WiFi signals when propagating through the material.

The authors in Nelson et al. (2002) showed that the dielectric constant and the loss factor are affected by the moisture content of wheat. Therefore they can serve as an indicator of moisture content in grains. In particular, the dielectric constant can be indirectly utilized to determine whether the grain is mildewed or not by moisture. However, the technique in Komarov et al. (2005) requires an expensive and customized equipment to detect the dielectric constant, which hinders the wide deployment of this technique in the field. In contrast, we propose to leverage off-the-shelf WiFi devices to detect wheat mildew, which is low-cost and easy to deploy. In particular, as the WiFi signal propagates through the wheat sample, the strength of the electric field will vary along with the distance to the wheat surface. This effect will be captured by the attenuation factor  $\alpha$  of the dielectric properties of grain,

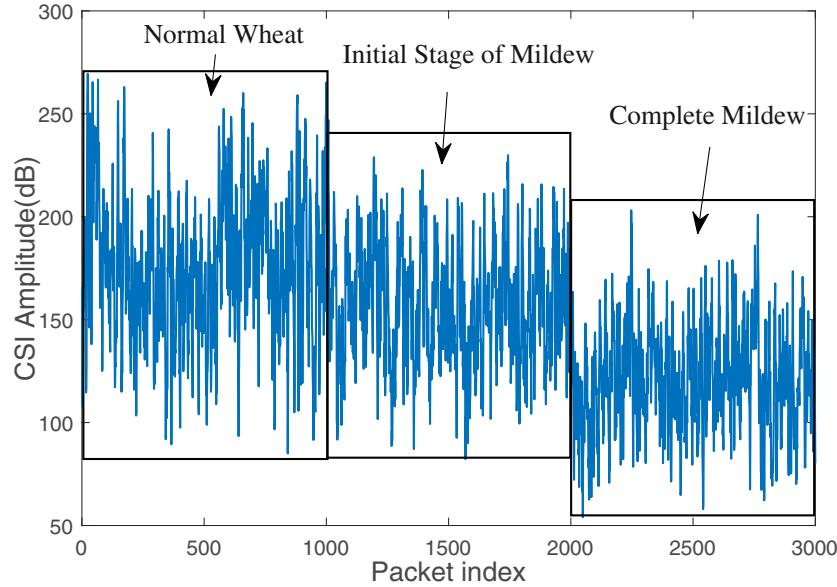


Fig. 1. CSI raw amplitude samples measured from the same wheat sample that is developing mildew through the three states: normal, initial state, and complete state.

which can be written as Komarov et al. (2005):

$$\alpha = \frac{2\pi}{\lambda_0} \sqrt{\frac{\epsilon'}{2} \left( \sqrt{1 + \left(\frac{\epsilon''}{\epsilon'}\right)^2} - 1 \right)}, \quad (2)$$

where  $\lambda_0$  represents the wavelength of the WiFi signal.

As mildew is developed in store wheat, i.e., from the normal state to the initial state, and eventually to the complete state, both the temperature and moisture level of the wheat will increase, as well as the humidity of the surrounding environment. Such variations will then cause changes in both the dielectric constant  $\epsilon'$  and dielectric loss factor  $\epsilon''$ . According to the relationship in (2), the attenuation factor  $\alpha$  will also be affected, since  $\alpha$  is a function of  $\epsilon'$  and  $\epsilon''$ . Eventually, the electric field, i.e., the WiFi channel, and the received WiFi CSI data will be influenced. Since the CSI can capture such changes in the electric field, we can detect the mildew state of the wheat sample by analyzing the WiFi CSI amplitude data. With such an approach, no expensive equipment is needed to measure the dielectric constant (i.e., by utilizing low-cost WiFi devices).

## 2.2. Wifi channel state information

As discussed, open-source device drivers for certain WiFi NICs allows collection of CSI samples from the OFDM subcarriers. Assume there are  $N_s$  subcarriers, Each measured CSI sample comprises the amplitude and phase of the subcarrier experienced by the corresponding received packet. The overall captured data consists of the number of transmitting antennas  $N_{tx}$ , the number of receiving antennas  $N_{rx}$ , the channel frequency  $f$ , and CSI data  $\mathbf{H}$ . The captured CSI data  $\mathbf{H}$  is in the form of an  $N_{tx} \times N_{rx} \times N_s$  tensor, which is given by

$$\mathbf{H} = (H_{ijk})_{N_{tx} \times N_{rx} \times N_s}. \quad (3)$$

Our implementation of MiFi is based on the Atheros AR5BHB NIC Xie et al. (2018), which allows sampling from the 56 subcarriers of the 20 MHz WiFi channel. The  $k$ th subcarrier in  $\mathbf{H}$  corresponding to a specific transmitting and receiving antenna pair can be expressed as

$$H_k = |H_k| \cdot e^{j\angle H_k}, \quad (4)$$

where  $|H_k|$  is the amplitude on the subcarrier and  $\angle H_k$  is the phase on the subcarrier.

## 2.3. Feasibility

In our recent work Yang et al. (2018a,b), we developed the Wi-Wheat system for detecting wheat moisture using commodity WiFi. This work is different from Wi-Wheat since wheat mildew does not only change the moisture level, but also the temperature of the wheat, as well as the air humidity of the surrounding environment, which then affects the WiFi propagation environment. Through extensive experiments, we verify that wheat mildew does affect the propagation of WiFi signals. To validate the feasibility of using WiFi CSI for detecting the mildew state of wheat samples, we measure CSI amplitude samples from the same wheat sample, which develops mildew through the three stages, while the WiFi transmitter, receiver, and wheat sample is placed at the same locations in the same environment. The measured CSI amplitude samples are plotted in Fig. 1, for the three mildew states, i.e., normal stage, initial stage of mildew, and complete stage of mildew. We observe from the figure that the CSI amplitude only changes slightly when the mildew state develops from normal to the initial stage. However, the CSI amplitude samples are significantly different when mildew further develops from the initial state to the complete state. Therefore, it can be concluded that WiFi CSI amplitude data can be useful for wheat mildew detection.

## 3. Design of the proposed mifi system

The architecture of the proposed MiFi system is presented in Fig. 2, which comprise four major modules: (i) the sensing module, (ii) the preprocessing module, (iii) the detection modeling module, and (iv) the mildew detection module. The detailed design of each of these modules are provided in this section.

### 3.1. Measure CSI amplitude samples

First, we utilize the Atheros AR5BHB NIC to collect CSI data from the 56 subcarriers of the WiFi OFDM channel, by transmitting multiple WiFi packets through wheat samples placed in the middle. In order to experiment with the initial stage of mildew and complete mildew conditions, we cultivate mildew in the same wheat examples. To accelerate the development of wheat mildew, a closed chamber with temperature and humidity control capability is used. For the experiments reported in

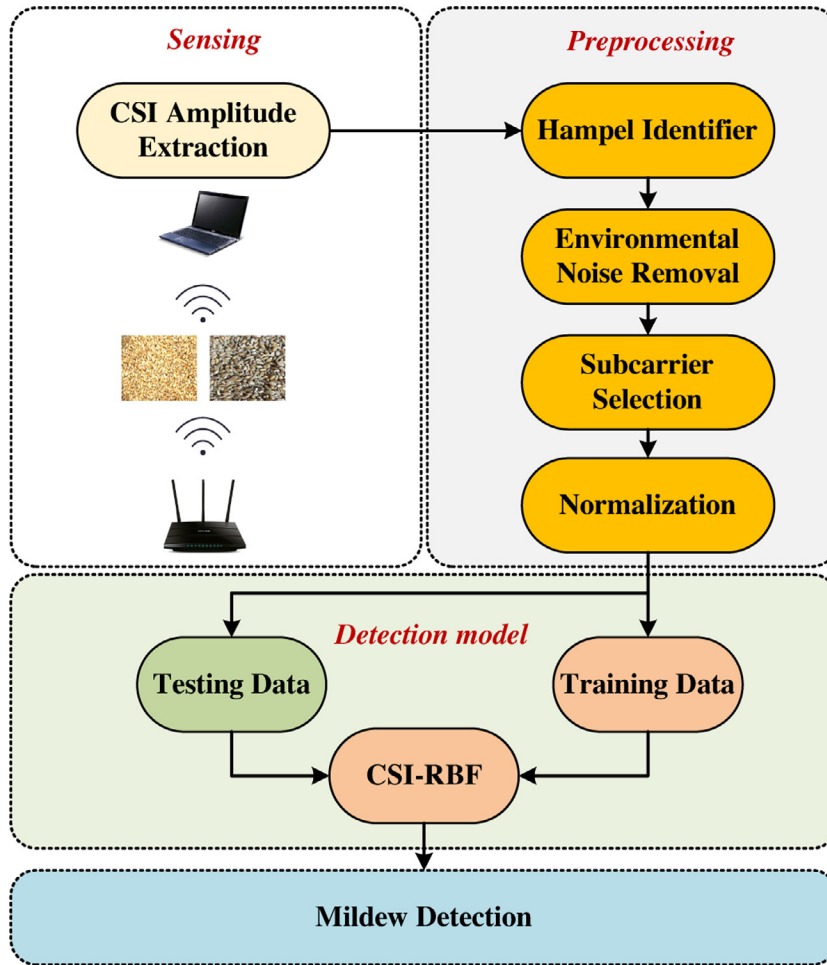


Fig. 2. The system architecture of the proposed MiFi system.

this paper, the temperature is maintained at 30 °C and the air humidity is maintained at 90%. After 2 to 3 days, the wheat will begin to grow mildew. Thus samples are obtained in the initial stage of mildew, and are used in our experiments. Then we let the mildew continue to develop in the same samples. Complete mildew samples will be obtained on the 8th day, and are used in our experiments. In this way, three types of CSI amplitude data will be obtained, one for each mildew stage, for our experimental study of detecting different wheat mildew stages.

### 3.2. Hampel identifier

The collected WiFi CSI data is usually noisy with outliers. Fig. 3 plots the CSI amplitude samples measured on the 20th subcarrier of the OFDM channel, where many outliers, indicated by the high peaks and low valleys, can be observed. Such outliers should be removed to avoid their effect on the detection performance. In our MiFi system, we incorporate a Hampel filter to detect and remove such outliers in measured WiFi CSI data.

In particular, the Hampel filter comprises a sliding window on the data from each subcarrier to eliminate the outliers. A CSI amplitude series with  $K$  samples captured from a specific subcarrier can be denoted as  $(Y_1, Y_2, \dots, Y_K)$ , where  $Y_i$  is the  $i$ th sample of CSI amplitude measured from the subcarrier. Let  $Y'$  be the median of the sequence of samples. The Hampel identifier classifies a sample  $Y_i$  as abnormal, if the sample deviates from the median absolute difference (MAD) more than a predefined threshold, as

$$\begin{cases} |Y_i - Y'| > l \cdot R, & \text{outlier} \\ |Y_i - Y'| \leq l \cdot R, & \text{normal,} \end{cases} \quad i = 1, 2, \dots, K, \quad (5)$$

where  $l$  is the predefined threshold value and  $R$  is the MAD, which is defined as

$$R = 1.4286 \times \text{MED}\{|Y_i - Y'|, i = 1, 2, \dots, K\}, \quad (6)$$

where  $\text{MED}(\cdot)$  returns the median value. In (6), the coefficient 1.4286 makes sure that the expected value of  $R$  be equal to the standard deviation of the data, which is assumed to be Gaussian Pearson (2002). In Fig. 3, the calibrated CSI amplitude data after Hampel filtering is also plotted. It can be seen from the figure that the outliers in the CSI data are effectively removed.

### 3.3. Remove the environmental noise

Although the outliers are removed by Hampel filtering, the resulting data is still noisy with environmental noise, which should be mitigated in order to achieve a high detection accuracy. In Fig. 4, we plot the spectrum of the CSI data measured from the 20th subcarrier for the three mildew states. It can be seen that the frequency variation caused by the wheat sample over a period of 15 seconds ranges from 0 Hz to 30 Hz. Based on this observation, we adopt a Butterworth filter to reduce the noise outside this band. The Butterworth filter uses a Butterworth function to define the amplitude-frequency characteristics in the pass-band. The low-pass mode squared function of the Butterworth filter used in MiFi is written as

$$|\mathcal{L}(f)|^2 = \frac{1}{(1 + (f/f_c)^{2n})}, \quad (7)$$



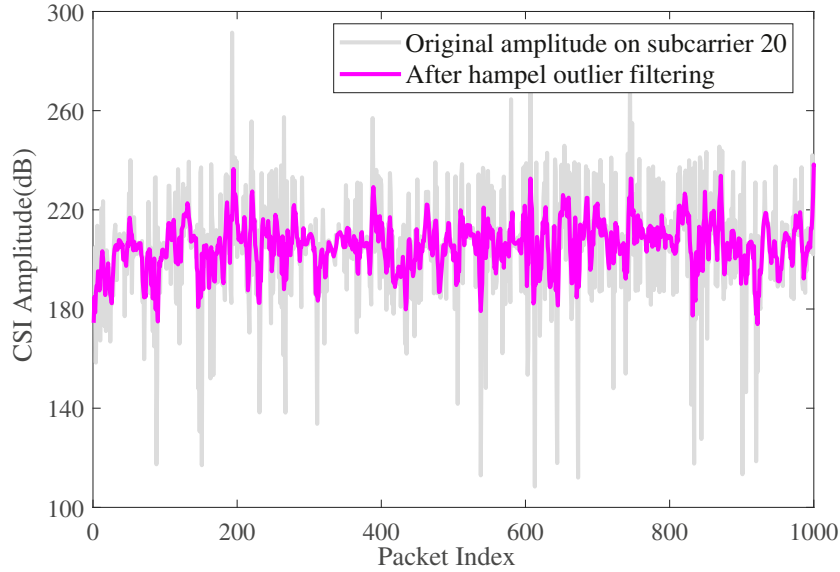


Fig. 3. Illustration of calibrating the WiFi CSI data measured from the 20th subcarrier.

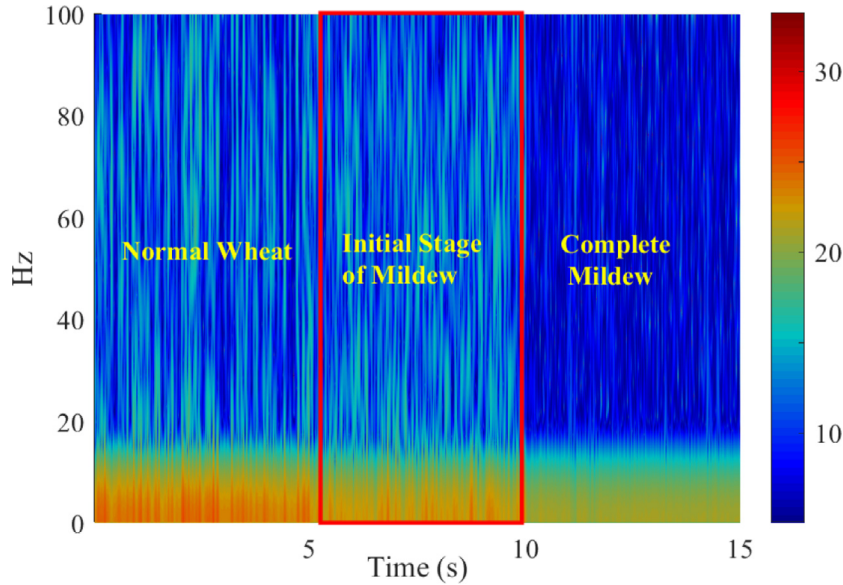


Fig. 4. Spectrum of the WiFi CSI data collected from the 20th subcarrier corresponding to the three mildew states.

where  $n$  is the order, and  $f_c$  is the cutoff frequency of the filter. In our MiFi implementation, we choose  $n = 4$  and set the cutoff frequency to 30 Hz (see Fig. 4).

### 3.4. Subcarrier selection

After denoising the CSI data, the CSI amplitude consists of a set of low frequency components. Through out experimental study, we also find that some subcarriers are more sensitive than others to the mildew state of the wheat samples. Specifically, we use the mean absolute deviation of CSI amplitude data from each subcarrier to characterize the sensitivity of the subcarrier Wang et al. (2017e). Generally speaking, the larger the mean absolute deviation, the higher the sensitivity. The sensitivity of the 56 subcarriers are plotted in Fig. 5. We observe from the figure that the subcarriers with an index below 35 (among the 56 subcarriers) are more sensitive (as indicated by the red area in the figure) to the mildew state of wheat samples. In MiFi, a more sensitive subcarrier is chosen (with an index below 35) in order to achieve a high detection accuracy.

### 3.5. Normalization of data

To speed up the computation of MIFI and achieve a high detection accuracy, the zero-mean normalization method (i.e., Z-score normalization) is applied in MiFi to normalize the calibrated CSI amplitude data. The normalized data  $\tilde{Y}_i$  is calculated by

$$\tilde{Y}_i = \frac{1}{\sigma} \cdot (Y_i - \bar{Y}), \tag{8}$$

where  $\bar{Y}$  is the mean, and  $\sigma$  is the standard deviation of the subcarrier's calibrated CSI amplitude data.

### 3.6. CSI-RBF Neural network

The normalized calibrated CSI amplitude data will be fed into a RBF neural network, termed CSI-RBF, to accurately detect the state of wheat mildew, and the K-means algorithm is used to set the parameters for the RBF kernel function.

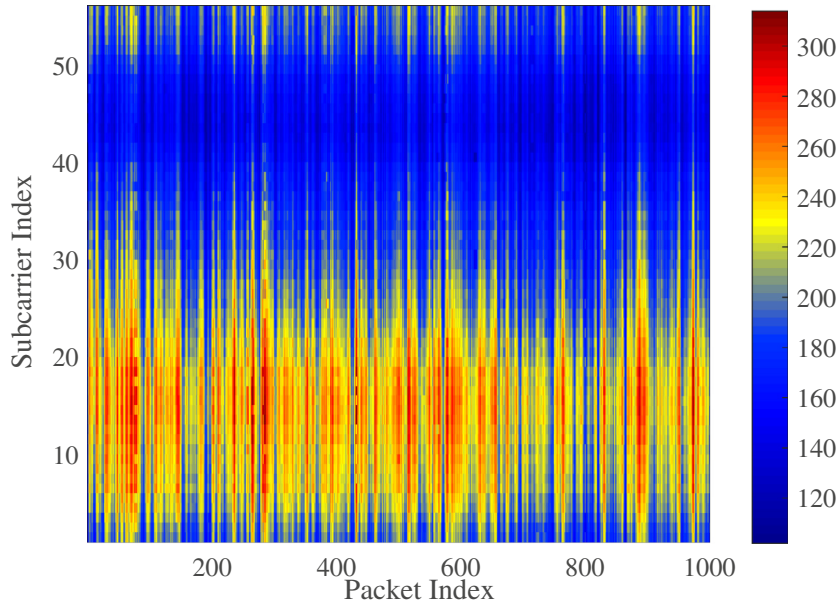


Fig. 5. CSI amplitude samples collected from each subcarrier after calibration, for selecting the most sensitive subcarrier.

### 3.6.1. K-Means clustering

K-means clustering is an unsupervised learning approach that has been widely used in many fields. In MiFi, K-means clustering is used to determine the parameters of a basis function and to determine the number of hidden neurons (which is equal to the number of clusters given by the K-means algorithm).

In the CSI-RBF model adopted in MiFi, the CSI amplitude sample sequences are clustered based on a similarity score, which is defined to be the Euclidean distance between the amplitude samples and the cluster center. The Euclidean distance between two CSI amplitude sequences  $\mathbf{V}^1$  and  $\mathbf{V}^2$  (in the form of two  $K$ -element time series) is computed by

$$D(\mathbf{V}^1, \mathbf{V}^2) = \sqrt{(V_1^1 - V_1^2)^2 + \dots + (V_K^1 - V_K^2)^2}. \quad (9)$$

### 3.6.2. CSI-RBF

RBF neural networks have the desirable capability of global approximation, by overcoming the shortcomings of slow convergence and local minima Johnson and Wichern (2002). Thus it is capable of modeling nonlinear relationships with fast convergence. Due to such advantages, we incorporate RBF neural networks in MiFi for rapid detection of wheat mildew states.

The MiFi system leverages the RBF neural network as a classifier. The basic structure of RBF consists of input neurons, hidden neurons, and output neurons, as shown in Fig. 6. In our MiFi design, the input layer is clustered and the CSI amplitude matrix  $\mathbf{V} = (V_1, V_2, \dots, V_q)$  is passed to the hidden layer with  $F$  hidden neurons. The hidden layer then maps the network inputs in a non-linear manner, with each hidden neuron connected to each cluster center and width. Multiple activation functions can be used in the hidden layer to maximize the accuracy of the output. In MiFi, the Gaussian function is adopted, given by

$$\theta(v) = e^{-\left(\frac{v-\gamma}{\beta}\right)^2}, \quad (10)$$

where  $v$ ,  $\gamma$ , and  $\beta$  are the input vectors, cluster center vectors, and hidden neuron widths obtained by K-means clustering Johnson and Wichern (2002). Here the number of hidden neurons is equal to the number of clusters.

The output layer implements a weighted sum linear function to the output of the hidden layer. The  $m = 3$  categories of wheat mildew states

are then detected. The linear function in the output layer is given by:

$$Z_m = y_m(w, v) = \sum_{j=1}^F w_{jm} \cdot \theta_j(v) + b, \quad (11)$$

where  $Z_m$  is the  $m$ th output neuron,  $w_{jm}$  is the weight from the  $j$ th hidden neuron to the  $m$ th output neuron,  $\theta_j(\cdot)$  is the  $j$ th Gaussian function in the hidden neuron, and  $b$  is the deviation. The CSI amplitude data collected from different mildew states are classified into  $m = 3$  categories. The weights between the hidden layer and the output layer can be easily determined by linear regression using the ordinary least squares (OLS) method.

### 3.7. Mildew detection

In the mildew detection module, the wheat mildew detection classification matrix is derived through the combination of linear and non-linear RBF neural network models, which is given by

$$\mathbf{Z} = [Z_1, Z_2, Z_3], \quad (12)$$

In (12), the  $Z_1$  vector is the output regarded as normal stage, the  $Z_2$  vector is the output regarded as initial stage of mildew, and the  $Z_3$  vector is the output regarded as complete mildew.

## 4. Implementation, experiments and discussions

### 4.1. Wheat preparation

We use real wheat samples in different stage of mildew development in our experiments. In Figs. 7(a) and 7(b), we show the normal wheat sample and the mildewed wheat sample, respectively. The sample shown in Fig. 7(b) was taken from the chamber with constant temperature and humidity on the eighth day, when the sample is completely mildewed. We measure the temperature and humidity inside both wheat samples. In addition, we employ a standard drying method to measure the moisture content of the wheat sample, which uses a high-speed universal pulverizer and an electrothermal constant temperature blast drying oven, as shown in Fig. 8.

During the experiments, we take three different types of samples of wheat with the same weight to test their mildew conditions, including the normal wheat sample, the sample in the initial stage of mildew, and

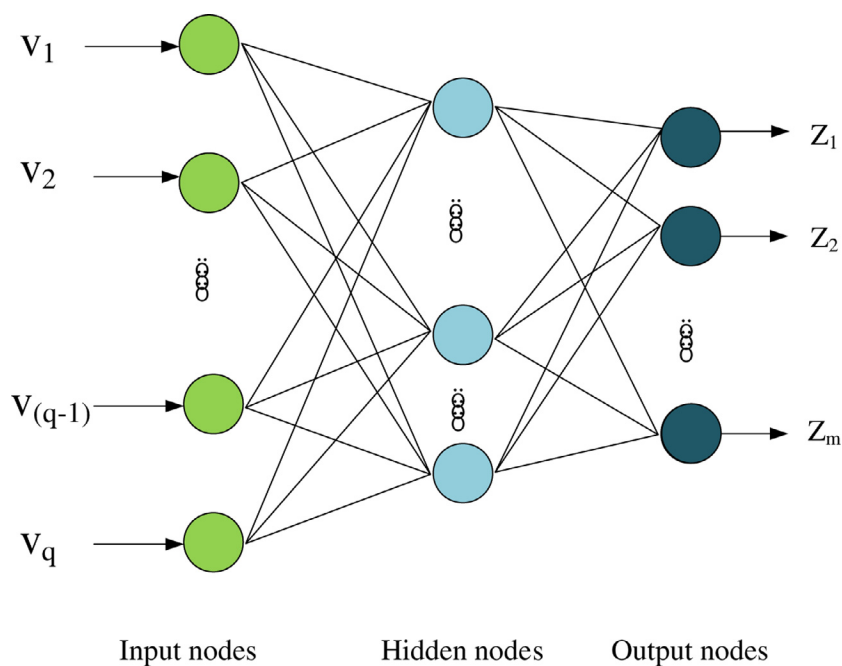


Fig. 6. The system architecture of the CSI-RBF neural network model.

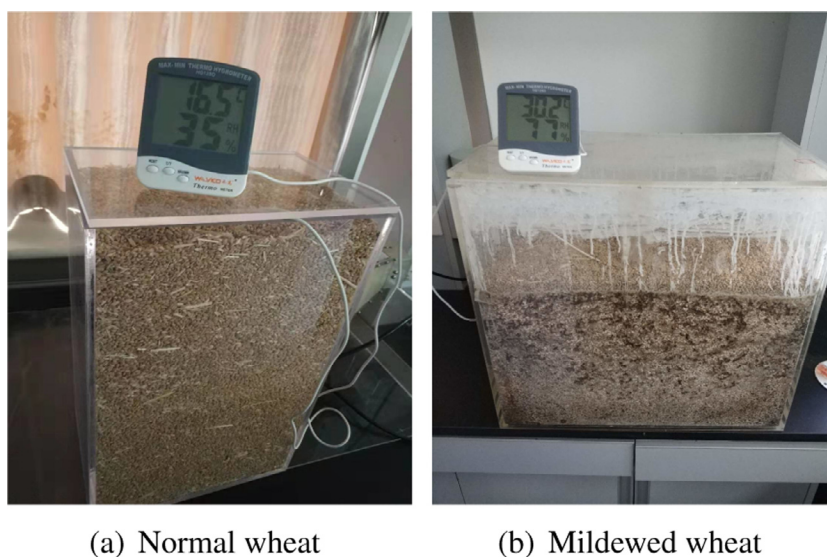


Fig. 7. The wheat samples used in our experiments.

**Table 1**  
Experimental Wheat Sample Conditions.

	Normal	Initial Stage of Mildew	Complete Mildew
Moisture	11.8%	12.9%	16.8%
Temperature	17 °C	20 °C	30 °C
Internal air humidity	32%	48%	77%

the sample in the complete stage of mildew. The water content, temperature, and humidity of the three types of wheat samples are provided in Table 2. It can be seen that the temperature, humidity, and internal air humidity of the wheat samples after mildew are all significantly increased.

**Table 2**  
Comparison between MiFi system and manual detection of wheat mildew.

Wheat Samples	MiFi (LOS)	MiFi (NLOS)	Manual Detection
1. Normal	✓	✓	✓
2. Normal	✓	✓	✓
3. Normal	✓	✓	✓
4. Initial Stage of Mildew	✓	×	×
5. Initial Stage of Mildew	×	✓	✓
6. Initial Stage of Mildew	✓	✓	✓
7. Initial Stage of Mildew	✓	×	×
8. Complete Mildew	✓	✓	✓
9. Complete Mildew	✓	✓	✓
10. Complete Mildew	✓	✓	✓



(a) The high speed universal disintegrator. (b) Electric thermostat blast drying oven.

Fig. 8. The oven-drying method for measuring the moisture content in wheat samples.



(a) The LOS scenario (b) The NLOS scenario

Fig. 9. Experimental configuration of the MiFi system.

#### 4.2. Implementation of the mi-Fi system

The prototype of MiFi is implemented using two Dell PP181 laptops equipped with Atheros AR5BHB NICs. One laptop serves as the transmitter using a single antenna, and the other laptop serves as a receiver using three antennas. Both laptops run the kernel 4.1.10 + 32-bit Ubuntu Linux 14.04 operating system and have 2 GB of RAM. The transmitter keeps on sending WiFi packets, while the receiver extract CSI samples for each received packet through the device driver.

We conduct extensive experiments in the Research Laboratory in the campus of Henan University of Technology, Zhengzhou, China. To test the effectiveness of the proposed MiFi system, experiments are carried out in both LOS and NLOS scenarios, which are shown in Figs. 9(a) and 9(b), respectively. In both cases, we place the transmitter and receiver on both ends of a bench, and different wheat samples in the middle for acquiring WiFi CSI data.

#### 4.3. Experimental results

Fig. 10 presents the detection accuracy of wheat mildew states in the LOS scenario. It can be seen that when the mildew state of the wheat sample is normal or completely mildewed, the MiFi system can achieve a detection accuracy of over 90% in both cases. Specifically, the detection accuracy is 91.34% and 92.6% for the normal and complete stages, respectively. When the wheat sample is in the initial stage of mildew, the detection accuracy of MiFi becomes lower than 90%. However, the detection accuracy in this case is 87.5%, which is still acceptable. We conclude that the MiFi system can accurately detect wheat mildew state in the LOS scenario.

Fig. 11 presents the detection accuracy results of wheat mildew detection in the NLOS scenario. It can be seen that when the state of the wheat sample is normal or completely mildewed, MiFi can achieve a detection accuracy of over 90% in both cases, which are 90% and 91.5%, respectively. When the wheat sample is in the initial stage of mildew,



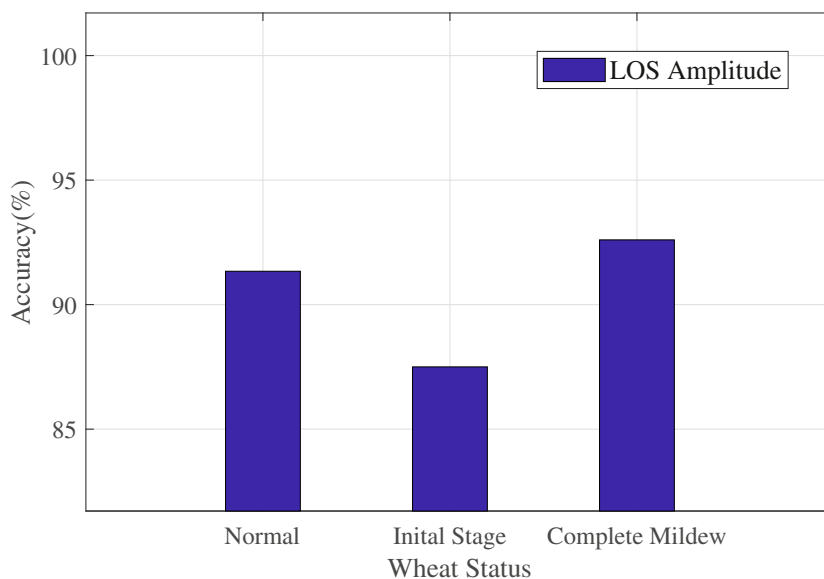


Fig. 10. Accuracy of wheat mildew detection under LOS scenarios.

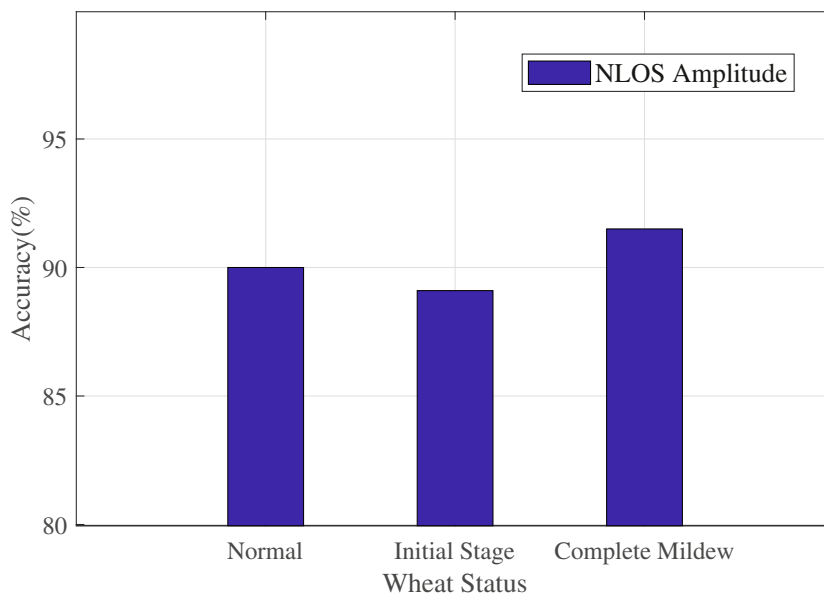


Fig. 11. Accuracy of wheat mildew detection under NLOS scenarios.

the accuracy of MiFi becomes lower than 90%, which is 89.1% and is still acceptable. We conclude that the MiFi system can effectively detect wheat mildew state in the NLOS scenario as well.

Present mildew detection is mostly based on manual operations (i.e., inspection by an expert). We compare the proposed MiFi system with manual wheat mildew detection to illustrate the effectiveness of our proposed method. Specifically, we prepared ten wheat samples, where three examples are normal, four samples are in the initial stage of mildew, and three samples are in the complete mildew stage. We first use the MiFi system to examine the samples in both LOS and NLOS scenarios. Then manual detection is executed for the ten samples. Table 2 presents the results of wheat mildew detection by MiFi and manual detection. The “√” sign indicates correct detection results, while the “X” sign indicates misdetection. Based on the results in the table, we find that both MiFi and manual detection are highly effective for both normal wheat and completely mildew wheat samples. For the samples in the initial stage of mildew, both MiFi and manual detection have

some misdetection results, since this mildew stage is much harder to detect.

From these experiments, we show that the proposed MiFi system is effective for detecting wheat mildew state in both LOS and NLOS scenarios, as well as achieving a performance comparable to manual detection by an expert.

#### 4.4. Impact of system parameters

We next examine the impact of MiFi system design parameters on the mildew detection accuracy. We examine the impacts of different transmit antennas, different distances between the transmitter and receiver, the spread parameter setting, the K-means algorithm, the CSI subcarrier selection, the ratio of training data to test data, the wheat sample container, and the antenna type.

We first examine the impact of using different antennas. Fig. 12 plots the average detection accuracy of achieved by using different an-

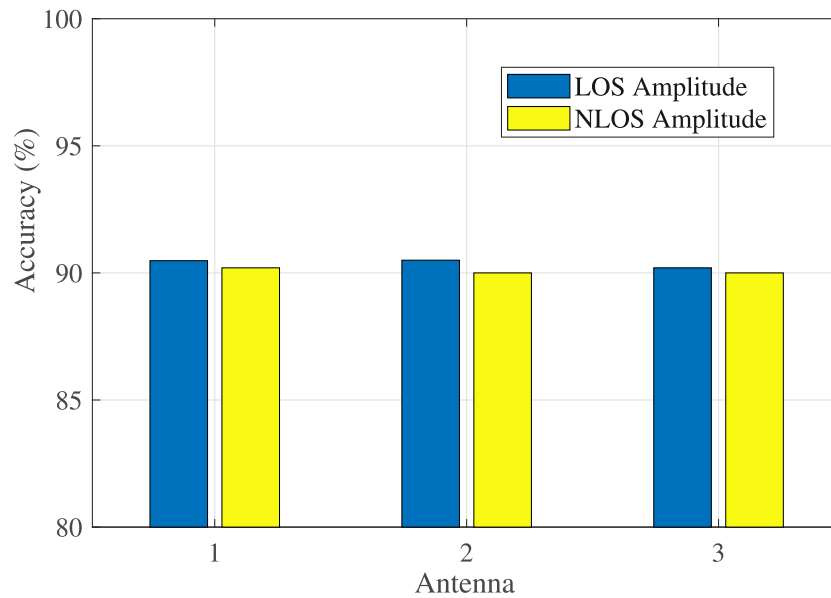


Fig. 12. Average detection accuracy for different antennas in LOS and NLOS scenarios.

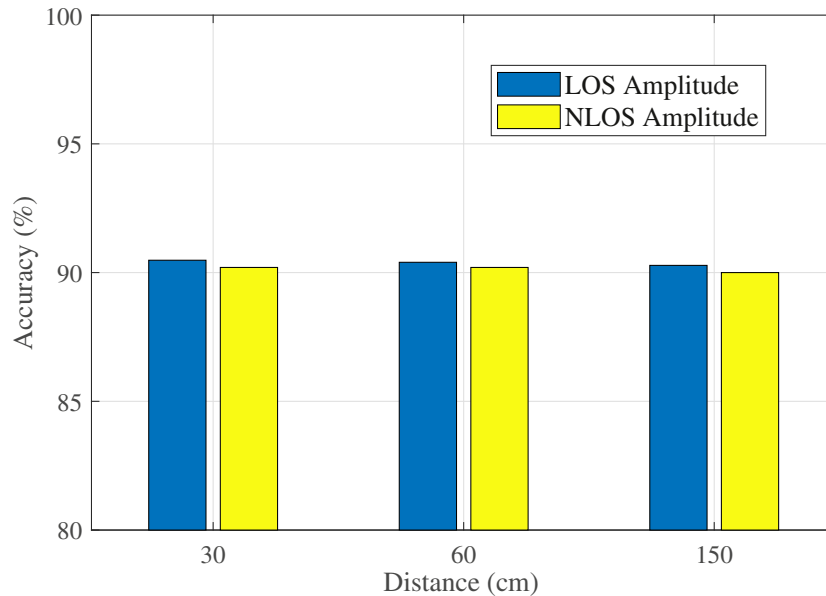


Fig. 13. Average detection accuracy over different transmitter-receiver distances.

tennas at the transmitter in the LOS and NLOS scenarios. Note that the receiver always uses three antennas to receive packets. The results show that the average mildew detection accuracy by using each of the three antennas is always higher than 90%. The difference in detection accuracy of using different transmit antennas is negligible, which evidence the robustness of MiFi. Using any of the transmit antennas in the MiFi system can effectively detect wheat mildew in both LOS and NLOS scenarios.

We next examine the mildew detection accuracy for different transmitter-receiver distances. Because the difference among the detection results of using the three transmit antennas is again very small, we only present the results using transmit antenna 1 as an example. Fig. 13 shows the average detection accuracy for different distances between the transmitter and receiver in the LOS and NLOS scenarios. It can be seen that for different distances in the range of 30cm to 150cm, the average detection accuracy using CSI amplitude data is very stable, and the detection accuracy of the MiFi system is always higher than 90%.

We also consider the impact of different spread parameter values in the RBF network on the detection accuracy. The larger the spread parameter value, the more the hidden neurons are needed, which will incur more computation. In addition, the smaller the spread parameter value, the worse the performance of the neural network. Thus, the best value needs to be tuned. Fig. 14 presents the average detection accuracy achieved by using different spread parameter values in the LOS and NLOS scenarios. We find that when the spread parameter is set to 3, the average detection accuracy will be the highest. When the spread value is less than 3 or greater than 3, the average detection accuracy of the system will drop below 90% in both cases. Therefore, the spread parameter value is set to 3 in the MiFi system.

Next, we study the impact of K-means clustering in the RBF network on the detection accuracy. Fig. 15 shows the average detection accuracy of the system with and without K-means clustering in the LOS and NLOS scenarios. The figure shows that, when K-means clustering is not used, the average detection accuracies in the LOS and NLOS scenarios drop to

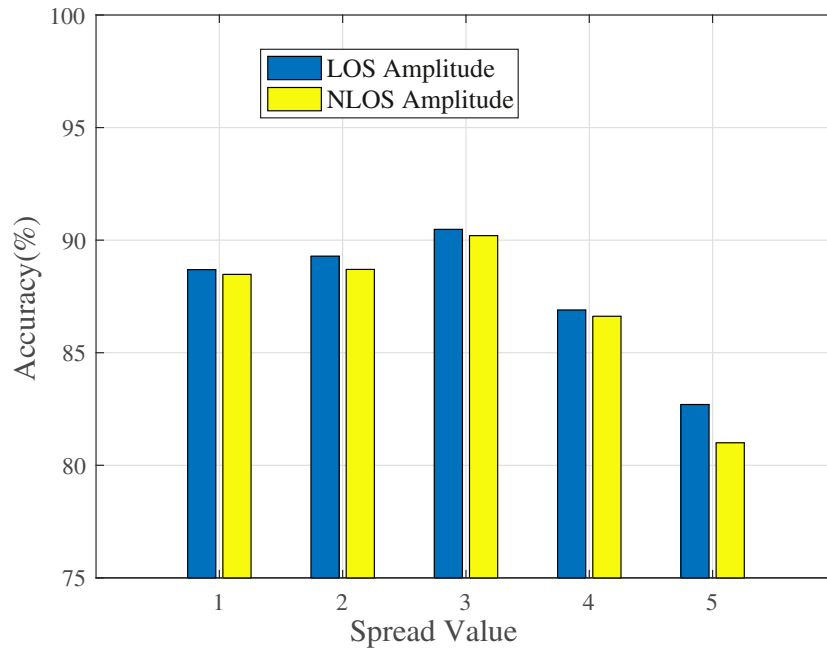


Fig. 14. Average detection accuracy achieved by using different spread parameter values in the LOS and NLOS scenarios.

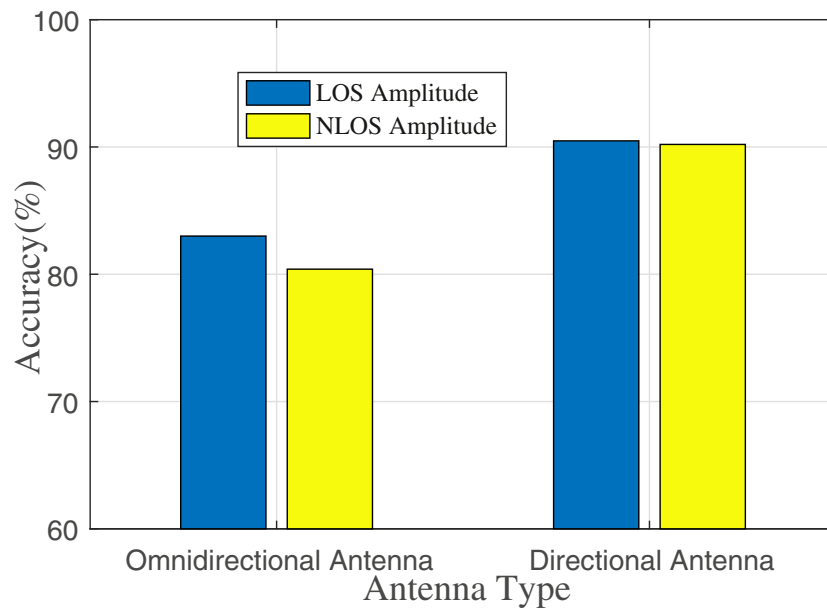


Fig. 15. Average detection accuracy of MiFi with and without  $K$ -means clustering in the LOS and NLOS scenarios.

74.75% and 73.49%, respectively, from the over 90% accuracy achieved when  $K$ -means clustering is used. Therefore  $K$ -means clustering can significantly improve the detection performance of the MiFi system.

In MiFi, the CSI data from the most sensitive subcarrier is selected and used for mildew detection. Fig. 16 presents the average detection accuracy achieved with or without subcarrier selection in the LOS and NLOS scenarios. The figure shows that the average detection accuracies without subcarrier selection are 82.74% and 80.95% in the LOS and NLOS scenarios, respectively. These are also much lower than the over 90% detection accuracy achieved with subcarrier selection. We conclude that subcarrier selection can significantly improve the detection accuracy of the system in both LOS and NLOS scenarios.

Since machine learning is used in MiFi, it is also interesting to examine the impact of the ratio of training data to test data. Fig. 18 shows

the average detection accuracy of different ratios of training data to test data in LOS and NLOS scenarios. When the ratio is 0.8, the average detection accuracies are higher than 90% in both cases. Specifically, the average detection accuracy is 90.48% in the LOS scenario and 90.2% in the NLOS scenario. When the ratio is lower than 0.7, the average detection accuracies in both the LOS and NLOS scenarios drop below 80%. Therefore the best ratio chosen in the MiFi system is 0.8.

In MiFi, the wheat samples are placed between the WiFi transmitter and receiver. In this experiment, we examine the impact the way the wheat samples are placed on the detection performance. Fig. 19 shows the average detection accuracy of different wheat containers in LOS and NLOS scenarios. When wheat is placed in an organic glass box and in a scattered heap, the corresponding average detection accuracies are both higher than 90%, while the detection accuracies are

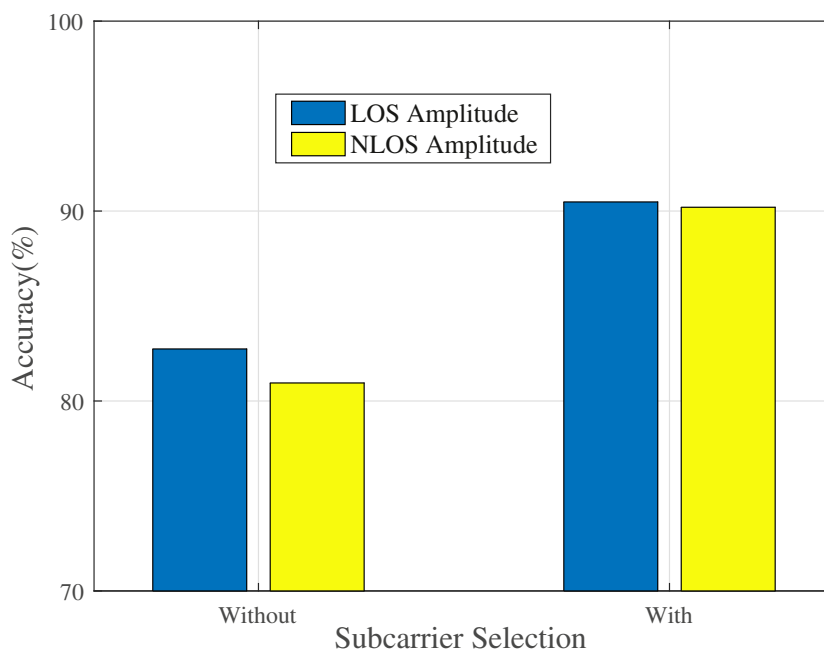


Fig. 16. Average detection accuracy of the CSI subcarrier selection and non-selection in the LOS and NLOS scenarios.

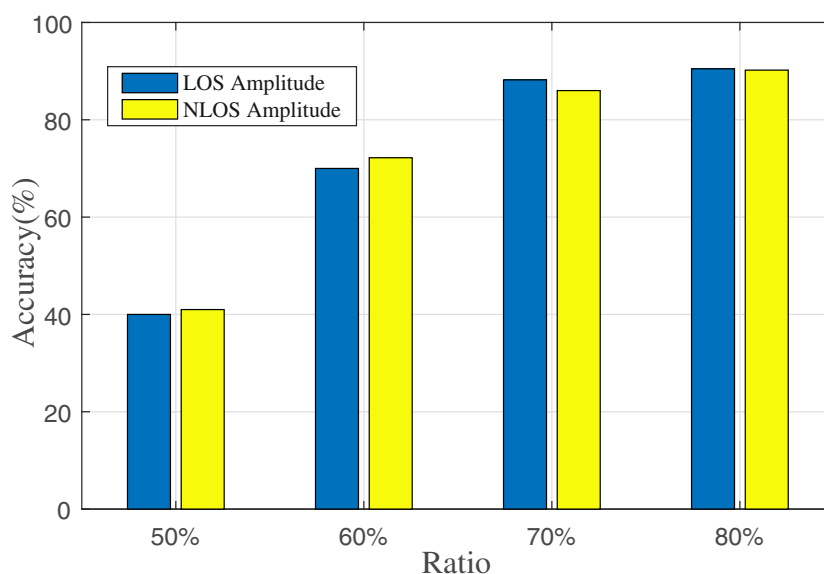


Fig. 17. Average detection accuracy with different ratios for training data over test data.

close to each other. When a paper box is used to hold the wheat sample, the average detection accuracy drops to 82.5% and 80.8% in the LOS and NLOS scenarios, respectively. Compared with the first two ways of placement, the result by using the paper box much worse. We can see that carton boxes have a negative impact on the MiFi system performance.

Finally, we investigate the impact of different types of antenna on the performance of wheat mildew detection. Fig. 20 shows the average detection accuracy of wheat mildew using different types of antenna in LOS and NLOS scenes, where omnidirectional antenna and directional antenna are used. From Fig. 20, it can be seen that when directional antenna is used, the average detection accuracy is higher than 90%, while when omnidirectional antenna is used, the average detection accuracy of wheat mildew drops to 83% and 80.4% in LOS and NLOS scenarios, respectively. The detection result of omnidirectional antenna is lower

than that of directional antenna, which is due to the fact that omnidirectional antenna is more vulnerable to interference from the environment, resulting in a degraded detection accuracy.

#### 4.5. Discussions and future work

The proposed MiFi system has been shown effective in a laboratory environment and is highly suited for detection of wheat samples. However, there are still uncertain factors need to be dealt with in the real, complex storage environment. First of all, it will be interesting to investigate how to deploy the system in the field. Due to the difference in size and shape of grain inventories in various regions, the gap between the real site environmental and the laboratory environment should be investigated and closed. Second, it is important to study the influence of the human body in the surroundings of the detec-



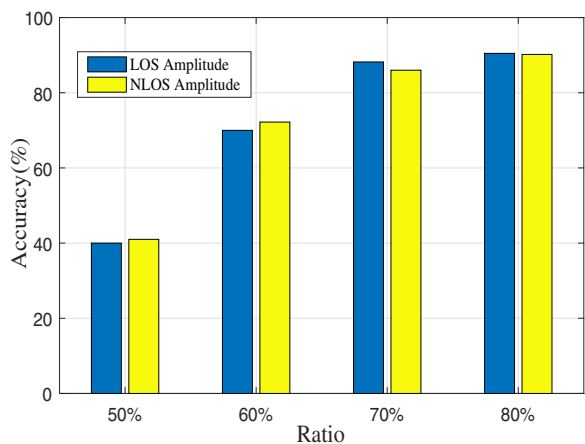


Fig. 18. Average detection accuracy with different ratios for training data over test data.

tion system, which introduces additional interference to the WiFi signal. Finally, it would be interesting to study the impact of pests in stored wheat. Usually the impact of the microbial pests on WiFi signal is very small and can be ignored. However, larger-sized pests, e.g., mice, will affect the propagation of WiFi signal. Note that the proposed scheme can also be leveraged to detect the presence of such larger pests.

Thus, interesting future work is needed on how to develop a WiFi based system for easy deployment in grain inventories, while robust mildew detection becomes an important problem. In our future work, we will consider several approaches to address the challenges of dynamic environments and human influence. The first method is to use adversarial domain adaptation to remove the influence of environment or human factors while extracting effective features of WiFi CSI for robust mildew detection. Second, we will consider few-shot learning or meta-learning to adjust the model parameters when applied to a new environment, using a small number of new samples Wang et al. (2021a). In addition, we will develop unsupervised methods (e.g., using a variational autoencoder) for detection of pest movements using WiFi CSI.

### 5. Related work

Mildew is one of the most critical causes of the damage in food security. Our work mainly is focused on mildew detection and WiFi-based contactless sensing. The related works in these two areas are discussed as follows.

#### 5.1. Mildew detection technology

Traditional mildew detection mainly relies on human manual operations through smelling and inspection to determine whether the grain is mildewed. This approach usually requires considerable manpower and time, and is subjective to the experience of the inspector. It has low efficiency and could be harmful to the human inspector. In addition, electronic noise sensors Zhang et al. (2007); Zhao et al. (2008), near-infrared spectroscopy Fernández-Ibañez et al. (2009), image processing Hong et al. (2007); Zhong-zhi et al. (2010) and other methods have also emerged. The electronic noise sensor method requires to deploy sensors into the food, which requires considerable manpower and incurs high cost. It is also costly to remove the malfunctioning sensors out of the grain. The use of near-infrared spectroscopy can effectively detect grain mildew, but near-infrared instruments are expensive and hard to be deployed in farms and operated by farmers. The image processing method requires a high-definition camera to achieve a satisfactory detection performance. This method is also hard to be deployed in the field. Only the surface of the grain pile can be captured by the camera, while the inner part of the grain pile, which is more likely to be mildewed, is invisible to the camera. Therefore, designing a real-time, non-destructive, and low-cost mildew detection system is of great value for food storage.

#### 5.2. Wifi-based contactless sensing

Recently, CSI-based sensing technologies have been applied in many fields such as indoor positioning, vital signs detection, and gesture and activity identification Wang et al. (2018). For indoor positioning, CSI has been widely utilized since it can provide fine-granular information of the propagation channel than RSS. The deep learning based schemes DeepFi Wang et al. (2015c, 2017b) and FIFS Xiao et al. (2012) leveraged CSI amplitude data, while PhaseFi Wang et al. (2015b, 2016b) and BiLoc

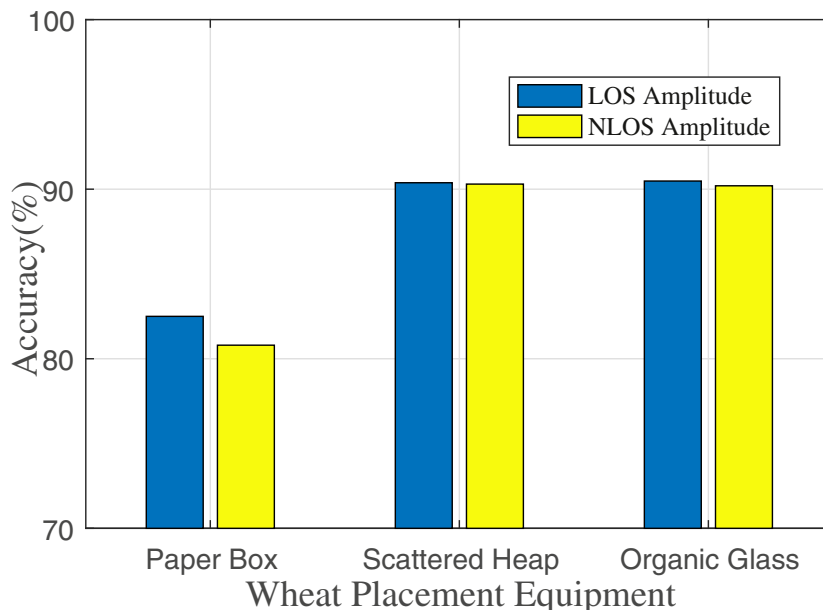


Fig. 19. Average detection accuracy using different wheat containers in LOS and NLOS scenarios.

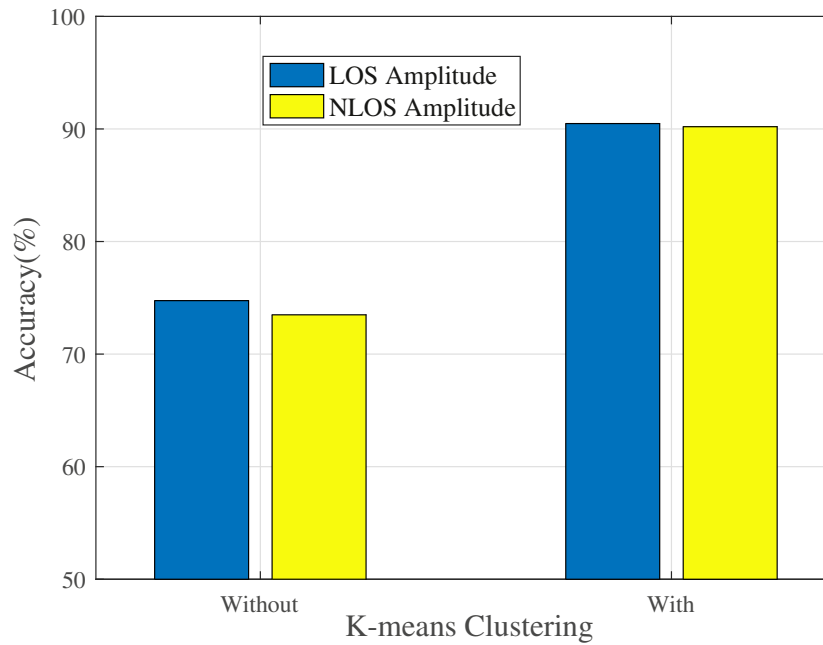


Fig. 20. Average detection accuracy for different antenna types in LOS and NLOS scenarios.

systems Wang et al. (2017a) utilized calibrated CSI phase data and dual-mode CSI data (AoA and amplitude), respectively. The GiFi system Wang et al. (2020, 2017c) and ResLoc system Wang et al. (2017d) used deep convolution networks and deep residual sharing learning for indoor localization, respectively, where CSI images and CSI tensors were used for learning the location features and for location estimation. In addition to indoor localization, CSI has also been used in RF sensing applications. For example, in vital signs monitoring applications, PhaseBeat Wang et al. (2021b, 2017e) and TensorBeat Wang et al. (2017g) used CSI phase different data to monitor the respiratory process of a single or multiple subjects. ResBeat was proposed for robust breathing monitoring using bio-modal CSI amplitude and phase difference data Wang et al. (2017f), which are complementary to each other. For activity recognition, RT-Fall Wang et al. (2016a) and WiFall Wang et al. (2017h) identified whether the patient falls or not using CSI phase difference and amplitude data, respectively. The E-eyes system Wang et al. (2014) and CARM system Wang et al. (2015a) utilized CSI data for activity recognition in indoor environment. The authors in Wu (2016) used CSI sensing technology to detect metal, while Wi-Fire Zhong et al. (2017) used CSI data to detect fire events. Recently, WiFi CSI have been leveraged for wheat moisture detection Yang et al. (2018a,b) as well as soil detection Ding and Chandra (2019). To the best of our knowledge, this is the first work that uses WiFi based contactless sensing for wheat mildew detection.

## 6. Conclusion

We proposed to use commodity WiFi for contact-free mildew detection for stored grain. In particular, we presented MiFi, a low-cost and non-destructive wheat mildew detection system based on WiFi CSI. We introduced the background of wheat mildew detection, and demonstrated the feasibility of wheat mildew detection using CSI amplitude data. We then presented the MiFi system design, including CSI data acquisition, data preprocessing, CSI-RBF detection modeling, and mildew detection modules. Our experimental results demonstrated the impact of various design parameters on the detection performance of the proposed MiFi system, and validated the high efficacy of MiFi, which achieved an average accuracy over 90% under both LOS and NLOS scenarios.

## Declaration of Competing Interest

The authors declare that they have no known competing financial interests or personal relationships that could have appeared to influence the work reported in this paper.

## References

- Ding, J., & Chandra, R. (2019). Towards low cost soil sensing using wi-fi. In *The 25th annual international conference on mobile computing and networking* (pp. 1–16).
- Fernández-Ibañez, V., Soldado, A., Martínez-Fernández, A., & De la Roza-Delgado, B. (2009). Application of near infrared spectroscopy for rapid detection of aflatoxin b1 in maize and barley as analytical quality assessment. *Elsevier Food Chemistry*, 113(2), 629–634.
- Halperin, D., Hu, W., Sheth, A., & Wetherall, D. (2010). Predictable 802.11 packet delivery from wireless channel measurements. In *Proc. ACM SIGCOMM 2010* (pp. 159–170). New Delhi, India
- Hong, C., Lirong, X., Xiaobo, H., Qiaohua, W., & Moucheng, W. (2007). Identification method for moldy peanut kernels based on neural network and image processing. *Transactions of the Chinese Society of Agricultural Engineering*, (4).
- Hu, P., Yang, W., Wang, X., & Mao, S. (2019). Mifi: Device-free wheat mildew detection using off-the-shelf wifi devices. In *Proc. IEEE GLOBECOM 2019, waikoloa, HI* (pp. 1–6).
- Jayas, D. S. (2012). Storing grains for food security and sustainability. *Springer Agricultural Research*, 1(1), 21–24.
- Jiang, H., et al., (2018). Smart home based on wifi sensing: A survey. *IEEE Access*, 6, 13317–13325.
- Johnson, R. A., Wichern, D. W., et al., (2002). *Applied multivariate statistical analysis*. Upper Saddle River, NJ: Prentice Hall.
- Komarov, V., Wang, S., & Tang, J. (2005). Permittivity and measurements. In K. Chang (Ed.), *Encyclopedia of RF and microwave engineering* (pp. 3693–3711). Hoboken, NJ: John Wiley & Sons.
- Lanier, C., Richard, E., Heutte, N., Picquet, R., Bouchart, V., & Garon, D. (2010). Airborne molds and mycotoxins associated with handling of corn silage and oilseed cakes in agricultural environment. *Elsevier Atmospheric Environment*, 44(16), 1980–1986.
- Magan, N., & Aldred, D. (2007). Post-harvest control strategies: Minimizing mycotoxins in the food chain. *Elsevier Int. J. Food Microbiology*, 119(1–2), 131–139.
- Nelson, S. O., Trabelsi, S., & Kraszewski, A. W. (2002). Principles of microwave moisture measurement in grain. In *Proc. IEEE IMTC 2002* (pp. 99–102). Anchorage, AK
- Nithya, U., Chelladurai, V., Jayas, D., & White, N. (2011). Safe storage guidelines for durum wheat. *Elsevier J. Stored Products Research*, 47(4), 328–333.
- Pearson, R. K. (2002). Outliers in process modeling and identification. *IEEE Transactions on Control Systems Technology*, 10(1), 55–63.
- Vasisht, D., Kapetanovic, Z., Won, J., Jin, X., Chandra, R., Sinha, S., Kapoor, A., Sudarshan, M., & Stratman, S. (2017). Farmbeats: An IoT platform for data-driven agriculture. In *Proc. USENIX NSDI 2017, boston, MA* (pp. 515–529).
- Wang, H., Zhang, D., Wang, Y., Ma, J., Wang, Y., & Li, S. (2016a). RT-Fall: A real-time and contactless fall detection system with commodity wifi devices. *IEEE Transactions on Mobile Computing*, 16(2), 511–526.

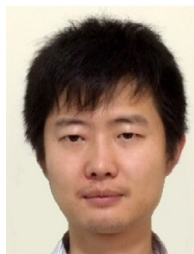
- Wang, L., Mao, S., Wilamowski, B., & Nelms, R. (2021a). Pre-trained models for non-intrusive appliance load monitoring. *IEEE Transactions on Green Communications and Networking*. 10.1109/TGCN.2021.3087702. To appear
- Wang, W., Liu, A. X., Shahzad, M., Ling, K., & Lu, S. (2015a). Understanding and modeling of wifi signal based human activity recognition. In *Proceedings of the 21st annual international conference on mobile computing and networking* (pp. 65–76). ACM.
- Wang, W., Wang, X., & Mao, S. (2020). Deep convolutional neural networks for indoor localization with CSI images. *IEEE Transactions on Network Science and Engineering*, 7(1), 316–327.
- Wang, X., Gao, L., & Mao, S. (2015b). Phasefi: Phase fingerprinting for indoor localization with a deep learning approach. In *Proc. IEEE GLOBECOM 2015* (pp. 1–6). San Diego, CA.
- Wang, X., Gao, L., & Mao, S. (2016b). CSI Phase fingerprinting for indoor localization with a deep learning approach. *IEEE Internet of Things Journal*, 3(6), 1113–1123.
- Wang, X., Gao, L., & Mao, S. (2017a). Biloc: Bi-modality deep learning for indoor localization with 5GHz commodity wi-Fi. *IEEE Access Journal*, 5(1), 4209–4220.
- Wang, X., Gao, L., Mao, S., & Pandey, S. (2015c). Deepfi: Deep learning for indoor fingerprinting using channel state information. In *Proc. IEEE WCNC 2015* (pp. 1666–1671). New Orleans, LA.
- Wang, X., Gao, L., Mao, S., & Pandey, S. (2017b). CSI-Based fingerprinting for indoor localization: a deep learning approach. *IEEE Transactions on Vehicular Technology*, 66(1), 763–776.
- Wang, X., Huang, R., Yang, C., & Mao, S. (2021b). Smartphone sonar based contact-free respiration rate monitoring. *ACM Transactions on Computing for Healthcare*, 2(2).
- Wang, X., Wang, X., & Mao, S. (2017c). Cifi: Deep convolutional neural networks for indoor localization with 5GHz wi-Fi. In *Proc. IEEE ICC 2017* (pp. 1–6). Paris, France.
- Wang, X., Wang, X., & Mao, S. (2017d). Resloc: Deep residual sharing learning for indoor localization with CSI tensors. In *Proc. IEEE PIMRC 2017* (pp. 1–6). Montreal, Canada.
- Wang, X., Wang, X., & Mao, S. (2018). RF Sensing for internet of things: A general deep learning framework. *IEEE Communications*, 56(9), 62–67.
- Wang, X., Yang, C., & Mao, S. (2017e). Phasebeat: Exploiting CSI phase data for vital sign monitoring with commodity wifi devices. In *Proc. IEEE ICDCS 2017* (pp. 1230–1239). Atlanta, GA.
- Wang, X., Yang, C., & Mao, S. (2017f). Resbeat: Resilient breathing beats monitoring with online bimodal CSI data. In *Proc. IEEE GLOBECOM 2017* (pp. 1–6). Singapore.
- Wang, X., Yang, C., & Mao, S. (2017g). Tensorbeat: Tensor decomposition for monitoring multi-person breathing beats with commodity wifi. *ACM transactions on intelligent systems and technology*, 9(1), 8:1–8:27.
- Wang, Y., Liu, J., Chen, Y., Gruteser, M., Yang, J., & Liu, H. (2014). E-Eyes: Device-free location-oriented activity identification using fine-grained wifi signatures. In *Proc. ACM mobicom 2014* (pp. 617–628).
- Wang, Y., Wu, K., & Ni, L. M. (2017h). Wifall: Device-free fall detection by wireless networks. *IEEE Trans. Mobile Comput.*, 16(2), 581–594.
- Wu, K. (2016). Wi-metal: Detecting metal by using wireless networks. In *Proc. IEEE ICC'16* (pp. 1–6). Kuala Lumpur, Malaysia.
- Xiao, J., Wu, K., Yi, Y., & Ni, L. M. (2012). FIFS: Fine-grained indoor fingerprinting system. In *2012 21st international conference on computer communications and networks (ICCCN)* (pp. 1–7). IEEE.
- Xie, Y., Li, Z., & Li, M. (2018). Precise power delay profiling with commodity wi-Fi. *IEEE Trans. Mobile Comput.*. To appear
- Yang, W., Wang, X., Cao, S., Wang, H., & Mao, S. (2018a). Multi-class wheat moisture detection with 5GHz wi-Fi: A deep LSTM approach. In *Proc. ICCCN 2018* (pp. 1–9). Hangzhou, China.
- Yang, W., Wang, X., Song, A., & Mao, S. (2018b). Wi-Wheat: Contact-free wheat moisture detection using commodity wifi. In *Proc. IEEE ICC 2018* (pp. 1–6). Kansas City, MO.
- Zhang, H., Wang, J., Ye, S., et al., (2007). Optimized of sensor array and detection of moldy degree for grain by electronic nose. *Chinese Journal of Sensors and Actuators*, 20(6), 1207–1210.
- Zhao, D.-A., Pan, T.-H., Zhu, J.-Y., & Wang, Q. (2008). Identification of grain mildew with ANN pattern recognition software based on VB and MATLAB. In *2008 IEEE international conference on networking, sensing and control* (pp. 808–811). IEEE.
- Zhong, S., Huang, Y., Ruby, R., Wang, L., Qiu, Y.-X., & Wu, K. (2017). Wi-fire: Device-free fire detection using wifi networks. In *Proc. IEEE ICC 2017* (pp. 1–6). Paris, France.
- Zhong-zhi, H., Yan-zhao, L., Jing, L., & You-gang, Z. (2010). Quality grade-testing of peanut based on image processing. In *2010 third international conference on information and computing: vol. 3* (pp. 333–336). IEEE.



**Pengming Hu** received his B.S. and M.S. degree both from the Zhengzhou University of Light Industry and Henan University of Technology, China, in 2016 and 2020, respectively. He worked in China Unicom from 2020 to 2021. Now, he is studying for the Ph.D. degree at Henan University of Technology, Zhengzhou, China. His interests focus on the application of wireless sensing and AI in wheat quality detecting. He is also interested in machine learning and optimization theory.



**Weidong Yang** received his B.S. in industrial automation, and M.S. and Ph.D. degree in Computer Science from Xidian University in China in 1999, 2005, and 2008, respectively. He is now a professor in Henan University of Technology, deputy chair of Key Laboratory of Grain Information Processing and Control (Henan University of Technology) ministry of Education. He is also a senior member of China Computer Federation (CCF). His research focuses on wireless networks security, privacy protection, and vehicular Ad Hoc networks.



**Xu Yu Wang** received the M.S. in Signal and Information Processing in 2012 and B.S. in Electronic Information Engineering in 2009, both from Xidian University, Xi'an, China. He received a Ph.D. in Electrical and Computer Engineering from Auburn University, Auburn, AL, USA in Aug. 2018. He is an Assistant Professor in the Department of Computer Science, California State University, Sacramento, CA. His research interests include wireless sensing, Internet of Things, wireless localization, smart health, wireless networks, and deep learning. He received the NSF CRII Award in 2021. He was a co-recipient of the Second Prize of the Natural Scientific Award of the Ministry of Education, China, in 2013, the IEEE Vehicular Technology Society 2020 Jack Neubauer Memorial Award, the IEEE GLOBECOM 2019 Best Paper Award, the IEEE ComSoc MMTc Best Journal Paper Award in 2018, the Best Student Paper Award from the IEEE PIMRC 2017, and the Best Demo Award from the IEEE SECON 2017. He was invited to organize a tutorial on CVPR 2020, a special session on IEEE BHI 2021, and to give a keynote speech on CVPm 2020. He is an associate editor of Digital Communications and Networks Journal. He is also an editor of Elsevier Book titled "Contactless Vital Signs Monitoring".



**Shiwen Mao** received his Ph.D. in electrical engineering from Polytechnic University, Brooklyn, NY in 2004. After joining Auburn University, Auburn, AL in 2006, he held the McWane Endowed Professorship from 2012 to 2015 and the Samuel Ginn Endowed Professorship from 2015 to 2020 in the Department of Electrical and Computer Engineering. Currently, he is a Professor and Earle C. Williams Eminent Scholar Chair, and Director of the Wireless Engineering Research and Education Center at Auburn University. His research interest includes wireless networks, multimedia communications, and smart grid. He is an Associate Editor-in-Chief of IEEE/CIC China Communications, an Area Editor of IEEE Transactions on Wireless Communications, IEEE Internet of Things Journal, IEEE Open Journal of the Communications Society, and ACM GetMobile, and an Associate Editor of IEEE Transactions on Cognitive Communications and Networking, IEEE Transactions on Network Science and Engineering, IEEE Transactions on Mobile Computing, IEEE Network, IEEE Multimedia, and IEEE Networking Letters, among others. He is a Distinguished Lecturer of IEEE Communications Society and a Distinguished Lecturer of IEEE Council of RFID. He was the TPC Co-Chair of IEEE INFOCOM 2018 and is the TPC Vice Chair of IEEE GLOBECOM 2022. He received the IEEE ComSoc TC-CSR Distinguished Technical Achievement Award in 2019 and NSF CAREER Award in 2010. He is a co-recipient of the 2021 IEEE Internet of Things Journal Best Paper Award, the 2021 IEEE Communications Society Outstanding Paper Award, the IEEE Vehicular Technology Society 2020 Jack Neubauer Memorial Award, the IEEE ComSoc MMTc 2018 Best Journal Award and 2017 Best Conference Paper Award, the Best Demo Award of IEEE SECON 2017, the Best Paper Awards from IEEE GLOBECOM 2019, 2016 & 2015, IEEE WCNC 2015, and IEEE ICC 2013, and the 2004 IEEE Communications Society Leonard G. Abraham Prize in the Field of Communications Systems. He is a Fellow of the IEEE.